

The Profile of the HeI $4\ ^3D, ^3F - 2\ ^3P$ ($\lambda = 447.15\text{ nm}$; $\lambda = 447.0\text{ nm}$) Spectral Line Emitted from a Low-Pressure Afterglow Plasma Submitted to a Magnetic Field of 10 Tesla

H. W. Drawin and J. Ramette

Association Euratom-CEA sur la Fusion, Département de Physique du Plasma et de la Fusion Contrôlée, Centre d'Etudes Nucléaires, Fontenay-Aux-Roses (France)

Z. Naturforsch. 34 a, 1051–1058 (1979); received May 2, 1979 *

Measurement of the HeI line at $\lambda = 447.15\text{ nm}$ during the recombination of a helium plasma in a magnetic field of induction $B = 10\text{ Tesla}$ by means of a multichannel analyzer system with spectral and temporal resolution showed a Stark-Zeeman broadened line with a superposed line structure. — There are sufficient experimental indications to conclude that this structure is due to molecular transitions, in agreement with the observations for magnetic field-free afterglow plasmas. At the lowest electron densities also some of the weaker Zeeman components of both the allowed and forbidden transitions probably contribute to the structure. The existence of Baranger-Mozer plasma satellites under our experimental conditions could not be confirmed. — We observed further a relatively strong electron density-dependent asymmetry in the intensities of the two main lateral Zeeman-Stark components of the allowed line.

1. Introduction

One of the most often studied spectral line of neutral helium is the line at $\lambda = 4471.48\text{ \AA}$ ($4\ ^3D - 2\ ^3P$) and its forbidden component at $\lambda = 4469.96\text{ \AA}$ ($4\ ^3F - 2\ ^3P$), due to its importance in astrophysical applications [1–2] for determining electron densities and helium abundances in star atmospheres and in the laboratory for checking Stark broadening theories [3–5] under well defined experimental conditions [6–12]. Also the formation of plasma satellites has been predicted [13] for this line and their measurement as a mean for measuring electric field fluctuations due to collective plasma oscillations has been proposed. The existence of such plasma satellites was confirmed by several authors [5]. The authors of Ref. [10] interpreted for their plasmas a similar line structure superposed on the HeI $4\ ^3D, ^3F - 2\ ^3P$ transition as being due to He_2 molecular lines. In all these studies magnetic fields were assumed to be absent or were sufficiently weak so that their influence on the line profile could be neglected. This restriction is not further allowed when the spectral lines are emitted from magnetized stars or from plasmas confined by a strong magnetic field. In addition to electron density-dependent

Stark broadening, the atoms are submitted to Zeeman effect which can lead to strong modification of the line shape compared to pure Stark broadening. This has been shown for the hydrogen lines both theoretically and experimentally; for a comprehensive list of references see [14].

Although a strong magnetic field — in addition to the usual electric microfield — complicates the theoretical calculation of line profiles it provides from the experimental side a possibility to check line broadening theories under completely different conditions. A further important point is that due to the magnetic splitting of the atomic levels the plasma satellites should be shifted correspondingly. Application of a magnetic field opens therefore an additional possibility to check the theoretical concept of the formation of plasma satellites.

For helium lines, theoretical calculations of complete line profiles due to combined Stark and Zeeman effect have not yet been performed. The only laboratory study of combined Stark and Zeeman broadening of a helium line is the one of Belland et al. [15] who measured the central part of the profile of the HeI transition $3\ ^3D - 2\ ^3P$ ($\lambda_0 = 587.6\text{ nm}$) for magnetic inductions of $B = 3, 4, 5$, and 7 Tesla and electron densities N_e ranging from $2 \cdot 10^{15}\text{ cm}^{-3}$ to $3.5 \cdot 10^{16}\text{ cm}^{-3}$.

There exist, however, both experimental and theoretical papers on combined Stark and Zeeman effect in *constant* electric and magnetic fields [16–22] for numerous singlet and triplet lines of helium. As far as the experimental work is concerned, the cor-

* Reception of the first version February 26, 1979.

Reprint requests to Mons. H. W. Drawin, Association Euratom-CEA, Département Fusion, Centre d'Etudes Nucléaires, Boite Postale N. 6, F-92260 Fontenay-Aux-Roses, Frankreich. 0340-4811 / 79 / 0900-1051 \$ 01.00/0

Please order a reprint rather than making your own copy.



Dieses Werk wurde im Jahr 2013 vom Verlag Zeitschrift für Naturforschung in Zusammenarbeit mit der Max-Planck-Gesellschaft zur Förderung der Wissenschaften e.V. digitalisiert und unter folgender Lizenz veröffentlicht: Creative Commons Namensnennung-Keine Bearbeitung 3.0 Deutschland Lizenz.

Zum 01.01.2015 ist eine Anpassung der Lizenzbedingungen (Entfall der Creative Commons Lizenzbedingung „Keine Bearbeitung“) beabsichtigt, um eine Nachnutzung auch im Rahmen zukünftiger wissenschaftlicher Nutzungsformen zu ermöglichen.

This work has been digitized and published in 2013 by Verlag Zeitschrift für Naturforschung in cooperation with the Max Planck Society for the Advancement of Science under a Creative Commons Attribution-NoDerivs 3.0 Germany License.

On 01.01.2015 it is planned to change the License Conditions (the removal of the Creative Commons License condition "no derivative works"). This is to allow reuse in the area of future scientific usage.

	B [Tesla]	Direction	F_0 [KV/cm]	N_e [cm^{-3}]
Foster [16]	0.27	$B \parallel F_0$	96	$1.3 \cdot 10^{17}$
Foster [17]	1.47	$B \parallel, \perp F_0$	8.5	$3.3 \cdot 10^{15}$
Foster and Pounder [18]	2.58	$B \perp F_0$	10 ... 131	$4.4 \cdot 10^{15} \dots 2 \cdot 10^{17}$
Steubing and Redepenning [19]	2.0	$B \perp F_0$	10 ... 50	$4.4 \cdot 10^{15} \dots 5 \cdot 10^{16}$
Steubing and Stolpe [20]	1.0 ... 3.2	$B \perp F_0$	1.2 ... 42	$1.8 \cdot 10^{14} \dots 3.8 \cdot 10^{16}$
Steubing and Lebowsky [21]	2.75	$B \parallel, \perp F_0$	6.5 ... 35.2	$2.5 \cdot 10^{15} \dots 3 \cdot 10^{16}$

Table 1. Experimental papers on Stark-Zeeman splitting in constant fields.

responding values of magnetic induction B and applied electric field strength F_0 have been summarized in Table 1. When the *constant* electric field F_0 applied in those experiments is put equal to the normal Holtsmark field strength

$$F_0 = 2.61 e_0 N_e^{2/3} \quad (1)$$

of the electric microfield of a plasma of electron density N_e one obtains the values listed in the last column of the table. In all those studies figured the $4^3\text{D}, 3^3\text{F} - 2^3\text{P}$ transition.

The essential results of the mentioned papers [16–22] with regard to the present work can be summarized as follows:

1. the line patterns have a complicated dependence on electric and magnetic field strengths. They are different for $\mathbf{F}_0 \parallel \mathbf{B}$ and $\mathbf{F}_0 \perp \mathbf{B}$;
2. as theoretically expected, the displacements of the components of the $4^3\text{D}, 3^3\text{F} - 2^3\text{P}$ transitions are asymmetric with respect to the position of the unperturbed line ($F_0 = 0, B = 0$) $4^3\text{D} - 2^3\text{P}$ and the intensities of the Stark-Zeeman components of the forbidden transition $4^3\text{F} - 2^3\text{P}$ increase with increasing F_0 ;
3. in the case of crossed electric and magnetic fields occur components corresponding to $\Delta m = \pm 2$ transitions, in addition to $\Delta m = 0, \pm 1$. This is especially the case for the $\Delta L = 2$ transition $4^3\text{F} - 2^3\text{D}$, see [18, 21].

According to these findings appreciable modifications of the line profile of the $\lambda = 4471 \text{ \AA}$ line can be expected when it is emitted from a plasma submitted to a sufficiently strong magnetic field. Further, for observation parallel to the direction of the magnetic field there should occur at least two pairs of plasma satellites situated at wavelength distances

$\pm \Delta \lambda_{\text{pe}}$ from the two Stark-Zeeman-shifted and broadened components of the forbidden line, provided these plasma satellites exist and are sufficiently excited. Detection of N_e -dependent peak positions according to

$$\Delta \lambda_{\text{pe}} = \pm (\lambda_0^2/c) \nu_{\text{pe}} \quad (2)$$

with the electron plasma frequency ν_{pe} given by

$$\nu_{\text{pe}} = \frac{1}{2\pi} \left(\frac{e_0^2 N_e}{\epsilon_0 m_e} \right)^{1/2} = 8.97 \cdot 10^3 N_e^{1/2} \text{ sec}^{-1} \quad (3)$$

(with N_e in cm^{-3}) would therefore be a strong support for the correctness of the theory of plasma satellites. Especially for the $\lambda_0 = 4471 \text{ \AA}$ line follows

$$\Delta \lambda_{\text{pe}} = \pm 5.817 \cdot 10^{-8} N_e^{1/2} \quad (4)$$

($\Delta \lambda_{\text{pe}}$ in \AA and N_e in cm^{-3}). For our experimental conditions ($N_e \approx 1.5 \cdot 10^{16} \text{ cm}^{-3} \dots 5 \cdot 10^{14} \text{ cm}^{-3}$) one would have $\Delta \lambda_{\text{pe}} \approx 7.2 \text{ \AA} \dots 1.31 \text{ \AA}$. It is to be mentioned that the plasma satellites should have line widths not smaller than the Stark-Zeeman broadened components of the forbidden transition $4^3\text{F} - 2^3\text{P}$.

2. Experimental

The line profiles were measured during the afterglow phase of a recombining pure helium plasma after short-circuiting of the plasma current. The experimental conditions are identical to those described in Ref. [10] apart from the fact that helium gas was used instead of hydrogen or a mixture of hydrogen and helium. Observation was in all cases along the axis of the discharge tube and, thus, parallel to the direction of the magnetic field.

In order to ensure that the Zeeman effect dominated the line pattern at the lowest electron densities for which precise intensity measurements were still

possible, we applied a magnetic induction $B = 10$ Tesla ($\leq 10^5$ gauss). The filling pressure was $p = 0.5$ Torr (spectroscopically pure helium).

For the line profile measurements we used a ten-channel spectrum analyzer system in connection with ten independent photomultipliers as described in Refs. [9, 10]. One channel covered a wavelength region of 0.1 Å. Since the intensities were displaced on ten oscilloscope screens with three different sensitivities it was possible to follow the evolution of the profile continuously.

3. Results

Figure 1 shows a number of measured line profiles at different times after short-circuiting of the plasma current. The electron densities measured with a helium-neon laser interferometer are given in the figure caption. The profiles exhibit the following characteristic features:

1. At early times, the line contour is broad and obviously dominated by Stark broadening. There occur some peaks especially in the line wings.
2. As time proceeds, two intense but still broadened components emerge in the central part accompanied by a number of weaker peaks. The wave-

length positions of the two most intense components change slightly with time and approach the theoretical value of $\Delta\lambda_z = \pm 0.936$ Å for the Zeeman components of the allowed transition $4^3D - 2^3P$ for $t \geq 100$ μs.

3. Simultaneously with the evolution of the profile in the central part there emerge many well-resolved peaks in the line wings. The intensities of the peaks change relative to each other in the course of time, but the peak positions stay practically constant.
4. In the course of time there is an inversion of the intensity ratio of the two intense components. They are differently broadened.
5. At the end of the afterglow one does not observe a simple Zeeman doublet — as one would expect for a measurement parallel to \mathbf{B} — but a complicated line pattern with a number of well resolved peaks.

4. Interpretation

In the following we will try to give a qualitative interpretation of the observed features. We begin with the peak structure in the outer parts of the line profiles.

On the blue side emerges an ensemble of six peaks between $\Delta\lambda \approx -5.5$ Å and $\Delta\lambda \approx -3.5$ Å. Within an uncertainty of one channel width (0.1 Å) their wavelengths correspond to those for known He_2 molecular lines shown in Fig. 10 of [10]. The characteristic structure between -4 Å and -3.5 Å also appeared in the afterglow of the magnetic field-free plasma (see Fig. 15 of Ref. [23]) for emission from the axial region but disappeared in the wall region (Fig. 8 of [10]). The presence of a magnetic field has little effect on molecular lines as will be discussed later.

All peaks occurring in Fig. 1 between $\Delta\lambda = -3.5$ Å and -3 Å have also been observed in a magnetic field-free afterglow plasma. Especially the strong peak at $\Delta\lambda = -3$ Å represents a characteristic feature in Figs. 4, 5 and 7 of [10]. Also the relatively intense peak at wavelength distance -2.4 Å ... -2.5 Å in Fig. 1 of the present paper appeared as a strong peak in the magnetic field-free afterglow (see Fig. 7 of [10]) at the same wavelength. It is to be noted that the peak at $\Delta\lambda = -4.3$ to -4.4 Å coincides with the generally strongest H_2

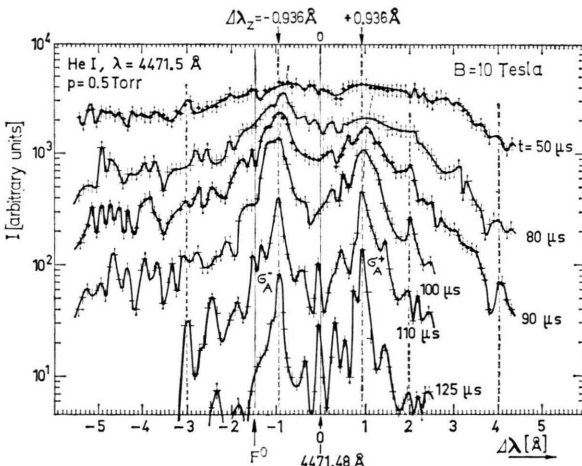


Fig. 1. Profiles of the HeI line $4^3D, 3F - 2^3P$ emitted by a helium afterglow plasma at different times t after short-circuiting of the plasma current. The magnetic induction is $B = 10$ Tesla. $\Delta\lambda = 0$ corresponds to $\lambda_0 = 4471.48$ Å. The arrow F° indicates position of the unperturbed $4^3F - 2^3P$ transition. The electron densities N_e are at $t = 50$ μs: $N_e \approx 1.5 \cdot 10^{16} \text{ cm}^{-3}$; $t = 80$ μs: $N_e \approx 5 \cdot 10^{15} \text{ cm}^{-3}$; $t = 90$ μs: $N_e \approx 3.3 \cdot 10^{15} \text{ cm}^{-3}$; $t = 100$ μs: $N_e \approx 2 \cdot 10^{15} \text{ cm}^{-3}$; $t = 110$ μs: $N_e \approx 1.4 \cdot 10^{15} \text{ cm}^{-3}$; $t = 125$ μs: $N_e \leq 5 \cdot 10^{14} \text{ cm}^{-3}$.

molecular line in that spectral region. However, due to the absence of a similarly strong H_2 line at $\Delta\lambda = +3.7 \dots 3.8 \text{ \AA}$ it is very likely that the intensities of possible H_2 molecular lines were too weak to be detected.

The red wings are less structured than the blue ones. There is nevertheless a great resemblance of the wing structures without and with magnetic field. Comparison of Fig. 7 in [10] with Fig. 1 of the present paper shows the same strong peaks at $\Delta\lambda \approx 4.0 \text{ \AA}$ and a relatively deep minimum at $\Delta\lambda \approx 3.8 \text{ \AA}$ in both cases. In the wavelength region $2.5 \text{ \AA} \dots 4 \text{ \AA}$ the curves for $t \leq 60 \mu\text{s}$ in Fig. 7 of [10] have great similarity with those for $t = 80 \mu\text{s}$ and $t = 90 \mu\text{s}$ in Fig. 1 of the present paper.

Within the experimental uncertainty the peaks between 1.5 and 2.5 \AA have the same wavelength positions without and with magnetic field.

In our paper [10] on magnetic field-free plasmas we interpreted the structure in the profile of the He atomic line as being due to He_2 molecular lines. The agreement of the peak positions without and with magnetic field leads to the conclusion that the peak structure has in both cases the same origin. There is no experimental indication for electron density-dependent peak positions according to Eq. (4) with $\Delta\lambda_{pe}$ measured from the Stark-Zeeman displaced components of the forbidden transition.

We have still to explain the structure of the central part of the line. We begin with the magnetic splitting

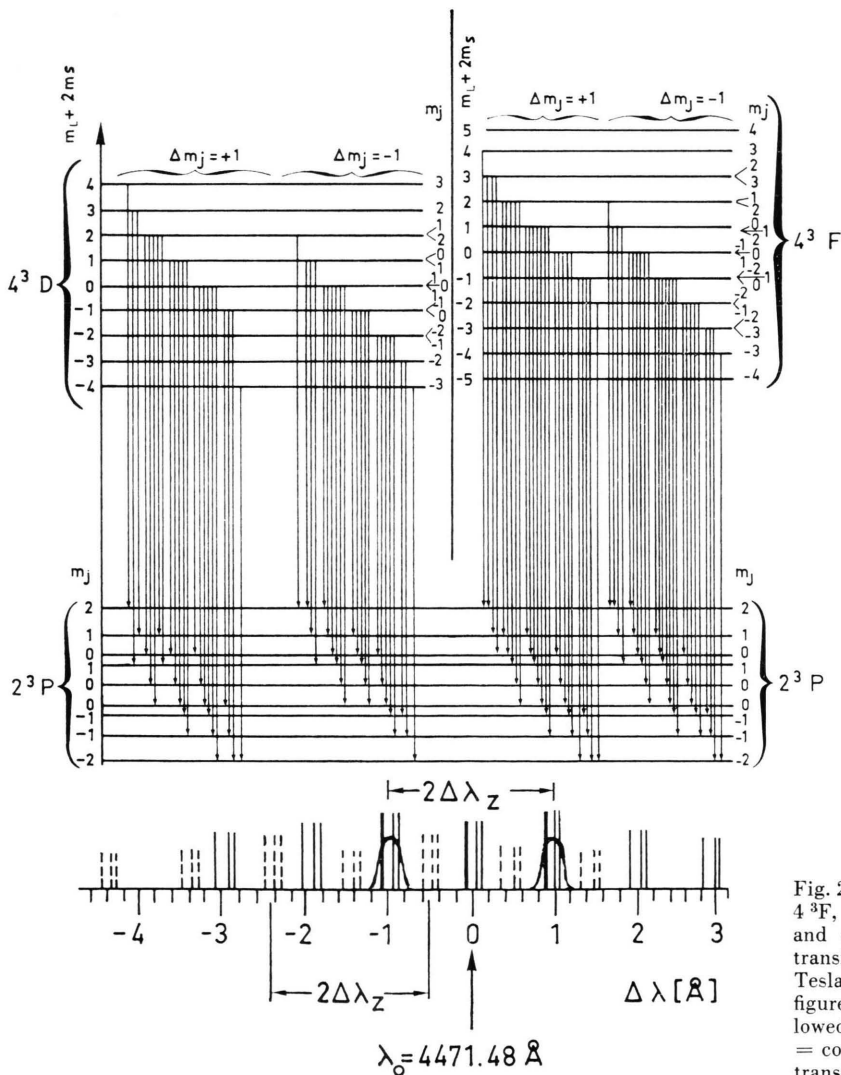


Fig. 2. Level splitting of the HeI states 4^3F , 4^3D and 2^3P in a magnetic field and components arising from $\Delta m_J = \pm 1$ transitions. The line pattern for $B = 10$ Tesla is shown in the lower part of the figure. Solid lines = components of allowed transitions $4^3D - 2^3P$; broken lines = components belonging to the forbidden transition $4^3F - 2^3P$.

of the 4^3D , 4^3F and 2^3P levels, neglecting for the moment Stark effect.

The magnetic splittings for $B = 10$ Tesla are shown in Figure 2. For the 2^3P level we have assumed intermediate Zeeman effect, i.e. the fine structure intervenes in the level splitting. Calculation of the sub-levels has been performed according to the method described in [24]. The level pattern of 2^3P corresponds qualitatively to the one in Fig. 24 of [24], but both the absolute and relative positions of the sub-levels are different, since we have a field of 10 Tesla instead of 0.85 Tesla in [24].

For the levels 4^3D and 4^3F we have assumed pure Paschen-Back effect (in Paschen-Back effect the fine structure splitting is neglected). The high magnetic field leads to a strong overlap of the two groups of sub-levels.

For emission parallel to the direction of the magnetic field the selection rule is $\Delta m_j = \pm 1$. For the allowed line there are 23 possible transitions for $\Delta m_j = -1$ and 23 transitions for $\Delta m_j = +1$. Some of them fall so close together that they cannot be distinguished from each other experimentally. One finally obtains seven groups of triplets as shown by the *solid* lines of the spectral line pattern in Figure 2. The lengths of the lines do not correspond to the intensities which have not been calculated.

Transitions between 4^3F and 2^3P with $\Delta m_j = \pm 1$ will lead to two times 26 components which also fall partly together. The resulting line pattern finally yields seven groups of triplets as shown by the *broken* lines of the spectral line pattern in Figure 2. If we allow for $\Delta m_j = \pm 2$ transitions (see introduction) we will obtain a further group of triplets to the left and to the right in addition to the already existing groups of triplets.

Let us assume that every component of a triplet is slightly broadened due to Stark effect and that each group of triplets actually appears as one line which has its intensity maximum at a mean wavelength position as it is shown in Fig. 2 for two groups. (In the frame of the spectral resolution of our device this is a sufficiently precise definition). One thus obtains a simplified Zeeman line pattern which is shown in Fig. 3 as “atomic lines”. The wavelength distance $\Delta\lambda = 0$ corresponds to the wavelength $\lambda = 4471.48 \text{ \AA}$ of the unperturbed transition $4^3D_{3,2} - 2^3P_{2,1}$.

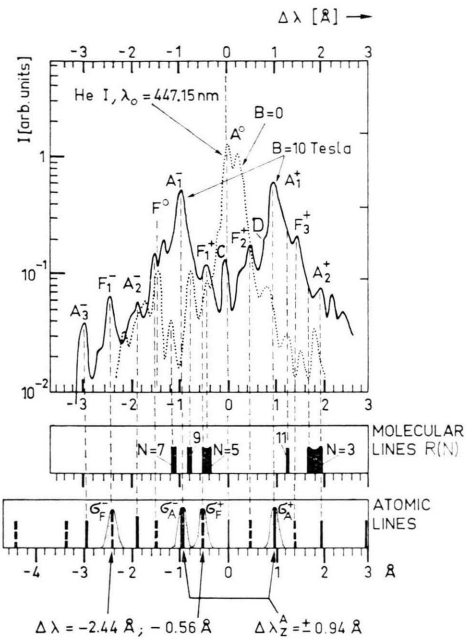


Fig. 3. The HeI line $4^3D - 2^3P$ without ($B = 0$) and with magnetic field ($B = 10$ Tesla). The peak structure is compared with He_2 molecular lines and with Zeeman components of the atomic transitions. For details, see text.

In Fig. 3 we compare this Zeeman line pattern with the peak structure of a line profile measured at low electron density. For this purpose we have drawn in the upper part of this figure the line profile measured at $t = 110 \mu\text{s}$ for $B = 10$ Tesla. In addition to this we show also the line profile for $B = 0$, published in Fig. 4 of [10]. A° represents the allowed line $4^3D - 2^3P$ and F° indicates the position of the forbidden transition $4^3F - 2^3P$ for $B = 0$, $N_e \rightarrow 0$. One sees that in the frame of our spectral resolution most of the measured peaks occurring at $B = 10 \text{ T}$ coincide either with the atomic Zeeman line pattern or with molecular lines at $B = 0$, or with both.

Let us first consider the Zeeman components of the *allowed transition*. The theoretical positions coincide with the measured maxima labeled A_3^- , A_2^- , A_1^- , A_1^+ , A_2^+ , but there is no measured peak exactly at $\Delta\lambda = 0$. We measured, however, a sharp well-resolved peak with a maximum at $\Delta\lambda = -0.1 \text{ \AA}$ labeled C in Figure 3. As can be seen from Fig. 1 the intensity of this peak relative to the one of the two most intense Stark-Zeeman components at $\Delta\lambda = \pm 0.94 \text{ \AA}$ increases with decreasing electron density. If C represents a Zeeman(-Stark) component, an inverse behavior is to be expected. We can therefore not exclude that C originates from a molecular tran-

sition. We already mentioned that a strong peak always occurred at $\Delta\lambda = -3.0 \text{ \AA}$ in the afterglow of a magnetic field-free plasma. We can thus not decide whether the peak A_3^- in Fig. 1 is a Zeeman component or not. Also the peaks A_2^- and A_2^+ have positions at which we measured peaks in the magnetic-field free afterglow plasma. These coincidences suggest that none of the peaks A_3^- , A_2^- , C and A_2^+ represents a "pure Zeeman(-Stark) component", it is more likely that they are all molecular lines or that they contain partly molecular intensities. Only the peaks labeled A_1^- and A_1^+ represent with certainty Zeeman-Stark components.

Next we consider the components of the *forbidden transition*. Some of the theoretical wavelengths coincide with measured peaks. This is the case for the maxima labeled F_1^- , F_2^+ and F_3^+ . However, there is no peak at the position F° , and the peak F_1^+ is obviously displaced by at least one channel width (0.1 \AA) to longer wavelengths with respect to the theoretical position of the Zeeman component at $\Delta\lambda = -0.56 \text{ \AA}$. If F_2^+ and F_3^+ represent Zeeman components the short wavelength analogues F_2^- and F_3^- should have been measured too. This is not the case.

These features and the fact that there still appear some other peaks and intensity shoulders (probably unresolved peaks) which do not coincide with theoretical wavelength positions of Zeeman components lead to the conclusion that the measured peak structure must – at least partially – have another origin than Zeeman(-Stark) effect of the allowed and forbidden atomic lines. A measurable influence of the electric microfield on the positions of the Zeeman components can probably be excluded at these low electron densities. It is very likely that also in the central part the peak structure is partly or entirely of molecular origin, as in the line wings.

Since both the atoms and molecules are submitted to the same strong magnetic field it is useful to remind briefly of the molecular Zeeman effect. Molecular lines show a complicated Zeeman effect which becomes relatively simple in the case of Paschen-Back effect. Assuming for He_2 Paschen-Back effect in Hund's case (b) one obtains for the energy splittings of a molecular level characterized by the quantum numbers A , K , M_k and M_s the formula (see e. g. page 152 in [25] or page 303 in [26])

$$\Delta E_{A, K, S} = \left[\frac{A^2 M_K}{K(K+1)} + 2 M_S \right] \frac{e_0 h}{4 \pi m_e c} B. \quad (5)$$

With the selection rules $\Delta M_S = 0$ and $\Delta M_K = \pm 1$ for Paschen-Back effect and observation parallel to the direction of the magnetic field it is easy to calculate the displacements of a rotational line. They rapidly decrease with increasing $K = A + N$, N being the rotational quantum number. In most cases one will observe a weakly broadened line instead of distinct Zeeman components (see also Fig. 146 in [26]). For the rotational lines of the $R(N)$ branch of the He_2 transition

$$\begin{aligned} 4 d\sigma j^3 \Sigma_u^+ (v' = 2, N' = N+1) \\ \rightarrow 2 p \pi b^3 \Pi_g (v'' = 2, N'' = N) \end{aligned}$$

the resulting molecular line pattern is shown in Fig. 3 for $N = 3, 5, 7, 9$ and 11 . For $N = 3$ there occur 9 Zeeman components, the displacement of the two outermost components is $\pm 0.187 \text{ \AA}$ with respect to the unperturbed $R(N=3)$ line. For $N = 11$, the 25 Zeeman components are spread over a wavelength region $\pm 0.068 \text{ \AA}$. (The $R(N=5)$, $R(N=7)$ and $R(N=9)$ lines have been identified in [10]).

One now sees that the peak labeled F_1^+ (which is broader than the peak C) coincides with the $R(N=5)$ molecular line rather than with the Zeeman component of the forbidden transition. It is very likely that F_1^+ actually originates from the superposition of the $R(N=5)$ He_2 molecular line and the Zeeman component of the forbidden transition in the He atom. Also the structure of the A_2^+ peak would be in agreement with this interpretation. The generally weaker lines with $N = 7, 9$ and 11 are probably masked by the much more intense Zeeman(-Stark) components A_1^- and A_1^+ .

The intensity shoulder D on the blue side of the A_1^+ component and the F_2^+ peak with its shoulder between C and F_2^+ coincide with the unresolved peaks labeled E_1 in Fig. 8 of Ref. [10] for a magnetic field-free afterglow plasma. Due to the fact that the line A° has been shifted to A_1^- , A_1^+ by the magnetic field the perturbing peaks are now resolved together with peak C which is completely masked by the allowed line when emitted by a magnetic field-free plasma. It is also seen that the shoulder D coincides with a resolved peak at $\Delta\lambda = 0.8 \text{ \AA}$ for the beginning discharge (curve $B=0$ in Fig. 3 of [10]).

Peaks at wavelengths for F_3^+ , A_2^- , and F_1^- have also been seen in the afterglow of a magnetic field-free plasma [10]. Even the peak just to the right of

F° , at $\Delta\lambda = -1.3 \text{ \AA}$, has been observed in the afterglow for $B=0$ (see Fig. 9 of [10]).

Thus — as far as the peaks are concerned — the two new features in the presence of a magnetic field are (1) : the peak just to the left of F° in Fig. 3 at $\Delta\lambda = -1.55 \text{ \AA}$ and (2) : the splitting of the allowed and forbidden transitions into the Zeeman-Stark components σ_A^- ($\cong A_1^-$), σ_A^+ ($\cong A_1^+$) and σ_F^- ($\cong F_1^-$), σ_F^+ ($\cong F_1^+$) respectively, with the restriction that F_1^- and F_1^+ are probably perturbed by molecular lines.

The other two important experimental features, namely a strong increase of the blue Zeeman-Stark component — compared with the red one — and the red-shift of both components with increasing electron density are easily explained by the increasing Stark effect of the electric microfield in connection with the Zeeman effect. Indeed, as can be seen from Fig. 3, the σ_A^- component of the allowed line at $\Delta\lambda_z = -0.94 \text{ \AA}$ and the σ_F^+ component of the forbidden transition at $\Delta\lambda = -0.56 \text{ \AA}$ lie relatively close together. Since the electric microfield mixes the wavefunctions of the 4^3D and 4^3F states the “forbidden transition” will increase its intensity with increasing N_e . The electric field also displaces the levels: the components belonging to the allowed and forbidden transitions will be shifted in opposite wavelength directions, namely σ_F^- , σ_F^+ to the blue side, the σ_A^- , σ_A^+ to the red one. (At a critical density N_e , the Stark broadened components σ_A^- and σ_F^+ would even fall together.) The overall effect will thus lead to an enhancement of the intensity on the blue side between -0.5 \AA and -1 \AA compared to the intensity on the red side between 0.5 \AA and 1 \AA when N_e increases. Simultaneously there must occur a red-shift of the two main intensity maxima, A_1^- and A_1^+ , in agreement with Figure 1.

It is worth mentioning that even at an electron density of $N_e \cong 1.5 \cdot 10^{16} \text{ cm}^{-3}$ (curve $t=50 \mu\text{s}$ of Fig. 1) the general form of the profile is quite different from the one measured at the same electron density in the absence of a magnetic field, although the Stark width of each individual transition $4^3D - 2^3D$ and $4^3F - 2^3P$ is larger than the Zeeman splittings. (Compare e.g. the curve for $t=50 \mu\text{s}$ in Fig. 1 with the profiles given in Ref. [12] for different N_e but without a magnetic field.) For a given N_e , the presence of a magnetic field obviously facilitates mixing of the wavefunctions and thus in-

creases the intensity of the “forbidden component”, compared to the magnetic field-free case.

We have searched for relations between wavelength positions of the peaks and combinations of plasma frequency and electron cyclotron frequency. No correlations between these quantities could be found.

5. Concluding Remarks

The essential results and conclusions are:

(i) As expected, a strong magnetic field leads to profound modification of the profile of the 4^3D , $3F - 2^3P$ transition of He compared to the magnetic field-free case. The gross line contour can qualitatively be explained by the combined action of electric and magnetic fields on the levels 4^3D , 4^3F and 2^3P . Quantitative comparison with theory was not possible, since line profile calculations do not exist for the experimental conditions investigated. Such a comparison would in any case have posed considerable difficulties due to an irregular peak structure superposed on the profile of the atomic line.

(ii) The intensities of the individual peaks change during the afterglow phase, their wavelengths, however, stay constant within the experimental uncertainty. Since we did not observe electron density-dependent wavelength positions of the peaks (an exception is the theoretically expected red-shift of the σ_A^- and σ_A^+ components in Fig. 1) we must conclude that the peak structure is not related to electron plasma waves. With the exception of two peaks, all have also been observed by us [10] in afterglow spectra of an unmagnetized plasma, or they coincide at low electron density with the theoretical predictions for the positions of the Zeeman components of both allowed and forbidden atomic transitions. It is thus very likely that those peaks which do not represent Zeeman components of the helium atom actually originate from molecular transitions.

In this context we would like to mention that PAL [27] observed under very different experimental conditions (initial phase of a theta-pinch generated plasma, $N_e \cong 5 \cdot 10^{12} \dots 1 \cdot 10^{14} \text{ cm}^{-3}$) quite a similar peak structure as we did for $B=0$ [10]. Although this sharp peak structure was not directly used for the evaluation of the turbulence level, its presence was attributed to non-thermal

field fluctuations. In our opinion the peak structure resulted from molecular transitions, as it might have been in other experiments too.

[1] A. Unsöld, *Z. Astrophys.* **23**, 75 (1944).

[2] A. Unsöld, *Physik der Sternatmosphären*, 2. Aufl. Springer-Verlag, Berlin 1955.

[3] H. R. Griem, M. Baranger, A. C. Kolb, and G. Oertel, *Phys. Rev.* **125**, 177 (1962).

[4] A. J. Barnard, J. Cooper, and W. Smith, *J. Quant. Spectrosc. Radiat. Transfer* **14**, 1025 (1974).

[5] H. R. Griem, *Spectral Line Broadening*, Academic Press, New York 1974.

[6] H. Wulff, *Z. Physik* **150**, 614 (1958).

[7] D. D. Burgess and C. J. Cairns, *J. Physics B* **4**, 1364 (1971).

[8] J. E. Jenkins and D. D. Burgess, *J. Phys. B* **4**, 1353 (1971).

[9] H. W. Drawin and J. Ramette, *Z. Naturforsch.* **29a**, 838 (1974).

[10] H. W. Drawin and J. Ramette, *Z. Naturforsch.* **33a**, 1285 (1978).

[11] R. Okasaka, M. Shimizu, and K. Fukuda, *J. Phys. Soc. Japan* **43**, 1708 (1977).

[12] C. Fleurier, G. Coulaud, and J. Chapelle, *Phys. Rev. A* **18**, 575 (1978).

[13] M. Baranger and R. Mozer, *Phys. Rev.* **123**, 25 (1961).

[14] H. W. Drawin and J. Ramette, *Z. Naturforsch.* **34a**, 1041 (1979).

[15] P. Belland, H. W. Drawin, and H. O. Tittel, *Z. Phys.* **222**, 372 (1969).

[16] J. S. Foster, *Proc. Roy. Soc. Lond. A* **122**, 599 (1929).

[17] J. S. Foster, *Proc. Roy. Soc. Lond. A* **131**, 133 (1931).

[18] J. S. Foster and E. R. Pounder, *Proc. Roy. Soc. Lond. A* **189**, 287 (1947).

[19] W. Steubing and W. Redepenning, *Ann. Physik Leipzig* **24**, 161 (1935).

[20] W. Steubing and F. Stolpe, *Ann. Physik Leipzig* **30**, 1 (1937).

[21] W. Steubing and I. Lebowsky, *Ann. Physik Leipzig* **7**, 360 (1959).

[22] C. Deutsch, H. W. Drawin, L. Herman, and Nguyen-Hoe, *J. Quant. Spectrosc. Radiative Transfer* **8**, 1027 (1968).

[23] H. W. Drawin and J. Ramette, Report EUR-CEA-FC-963, Investigation of the structure of the HeI 4^3D , $^3F - 2^3P$ ($\lambda = 447.15$ nm, $\lambda = 447.0$ nm) spectral line emitted from a low pressure plasma, Fontenay-aux-Roses 1978.

[24] H. A. Bethe and E. E. Salpeter, *Quantum Mechanics of One- and Two-Electron Systems*, in *Handbuch der Physik*, Vol. XXXV (Ed. S. Flügge), Springer-Verlag, Heidelberg 1957.

[25] W. Weizel, *Bandenspektren*, Akademische Verlagsgesellschaft, Leipzig 1931.

[26] G. Herzberg, *Molecular Spectra and Molecular Structure*, Vol. I: *Spectra of Diatomic Molecules*. Van Nostrand Reinhold Comp., New York 1950.

[27] R. Pal, Thesis 1978, University of Maryland; Investigation of non-thermal electric field fluctuations in a theta-discharge generated helium plasma using the forbidden transitions $2^{3,1}P - 4^{3,1}F$ of neutral helium, Technical Report No. 79-036, Department of Physics and Astronomy, University of Maryland 1979.

Acknowledgements

The technical help of Mr. E. Sablon is gratefully acknowledged.